

In situ optical second harmonic generation studies of electrochemical deposition of tellurium on polycrystalline gold electrodes

Ichizo Yagi ^a, Juliette M. Lantz ^b, Seiichiro Nakabayashi ^{a,c}, Robert M. Corn ^b,
Kohei Uosaki ^{a,*}

^a Physical Chemistry Laboratory, Department of Chemistry, Faculty of Science, Hokkaido University, Sapporo 060, Japan

^b Department of Chemistry, University of Wisconsin-Madison, 1101 University Ave., Madison, WI 53706, USA

^c PRESTO, Research Development Corporation of Japan

Received 26 May 1995; in revised form 14 July 1995

Abstract

The electrodeposition of tellurium (Te) on polycrystalline gold electrodes was studied using in situ optical second harmonic generation (SHG) at two different excitation wavelengths. On excitation at 1064 nm, the SH signal decreased dramatically with the first Te underpotential deposition (upd) and increased slightly with the second upd and the bulk deposition of Te. There was a linear correlation between the square root of the SH intensity from the surface and the surface coverage of Te, although the proportionality constant of this correlation for the first Te upd was different from those for the second upd and bulk deposition. This is possibly because of the stronger interaction of the first upd layer of Te than the second and bulk layer of Te with the substrate surface. However, on excitation at 585 nm, the behavior of the SH signal was more complicated, especially during the desorption process of the first Te monolayer. An increase in the SH intensity was observed with the first Te upd, but this increase in SHG still continued in the potential region in which no deposition of Te occurred. These results are interpreted by considering the existence of an optical resonance at the Au surface covered with a Te monolayer.

Keywords: Optical second harmonic generation; Electrochemical deposition; Tellurium; Polycrystalline gold electrodes

1. Introduction

Tellurium (Te) is one of the metalloids and has particularly interesting electronic properties. The adsorption of the metalloids may perturb the surface electronic properties of metal substrates quite differently from other metal adsorbates. Additionally, Te is an important component in the binary and ternary compound semiconductors, such as CdTe and HgCdTe. The thin film growth of CdTe on metal substrates has been extensively investigated to obtain stable surfaces with high light conversion yields. Electrodeposition has been one of the most studied methods [1–3], but there are problems in controlling the structure of the compound deposits. In order to control the resulting structure of the electrodeposited layers, a thorough knowledge of each deposited layer is required. Fortunately, the electrochemistry of tellurium has been investi-

gated in detail [4–8]. In addition, Stickney and coworkers [9–13] have carried out detailed characterizations of the first Te monolayer on Au single crystal surfaces by ex situ LEED and STM in order to establish the method of electrochemical atomic layer epitaxy (ECALE) of CdTe on well-characterized single crystal surfaces. They reported that ordered atomic layers of tellurium were formed on the low index planes of Au by repeating the underpotential deposition (upd) processes. Although structural information on electrodeposited Te layers has been partially obtained, the change in the surface electronic properties accompanying the upd process is not yet fully understood. The interactions between Te and metal substrates should play an important role in the thin film growth of compound semiconductors and should be interesting in view of the formation of metal|semiconductor interfaces.

Recently, surface second harmonic generation (SHG) has been recognized as a novel in situ optical probe of surface electronic and geometric structures [14–16]. Optical SHG is a second order non-linear optical effect that

* Corresponding author.

involves the conversion of two photons of frequency ω into a single photon of frequency 2ω . In the electric dipole approximation, this phenomenon requires a non-centrosymmetric medium. Therefore SHG cannot be observed in centrosymmetric media such as bulk metals and solutions. The SHG process can occur only within a few atomic layers on either side of the interface where inversion symmetry is broken. Consequently, the SH signal will be sensitive to changes at the surface and interface, therefore making this process a useful probe of various interfacial phenomena. This technique has been applied to various electrochemical systems, such as the adsorption of molecules, ions and metal atoms on metal and semiconductor electrodes [17–31]. Most of the recent SHG studies at metal electrodes, however, have investigated the structural properties of the surfaces and the adsorbed overlayers using rotational anisotropy measurements [19–23]. Although there have been several wavelength-dependent studies [25–31], these research efforts have focused on gaining an understanding of the correlation between the frequency dependence of SHG and the electronic properties of the metal substrate itself, and studies dealing with the adsorbate–substrate interaction are limited. Investigations of the electrodeposition of metals on different metal surfaces using linear spectroscopic methods [32–35] have indicated that the substrate–adsorbate interaction causes a frequency dependence of the optical responses. Thus different SH responses may be obtained during adsorption processes by varying the pump wavelength used in the SHG experiments. Buck et al. [31] reported that the SH signal from Au during alkanethiol adsorption was dependent on the pump wavelength. Further, it was reported that SH signal change, induced by the adsorption of certain species was observed only at specific fundamental wavelengths. For example, the adsorption of benzene on Rh(111) strongly attenuated 532 nm excited SHG, but hardly affected 1064 nm excited SHG [36]. If we can understand the frequency dependences of SHG in detail and optimize the wavelength conditions needed to study a surface or an adsorbate, SHG will become a more sensitive and therefore useful tool for interfacial studies.

In this article, we report the frequency-dependent behavior of the SH signal during tellurium electrodeposition on polycrystalline Au electrodes. We are interested in monitoring the Te upd process in real time using SHG measurements and in examining the change in the electronic structures of the Au surface brought about by the deposition of a Te monolayer. In this study, since we used polycrystalline Au, the SH signals reflect an averaged variation of the electronic properties of the surface. The SH intensity from Au surfaces changed with Te coverage and the magnitude of the changes was strongly wavelength dependent. The mass change at the surface caused by Te deposition was also studied by the electrochemical quartz crystal microbalance (EQCM) technique [37] to obtain useful information for understanding the SH response.

2. Experimental

Two different light sources were used to create SH signals on the electrode surface. Pulses (1.6 ps) of light (585 nm) generated by a 4 MHz cavity-dumped dye laser/mode-locked Nd:YAG laser system (Coherent model 702) were employed for visible excitation and 10 ns pulses of fundamental light (1064 nm) generated by a 10 Hz Q-switched Nd:YAG laser (LEXEL HY-200S) were employed for near-infrared excitation. The detailed experimental set-up used in the visible light excited SHG experiment has been described elsewhere [17,19,20]. For the near-infrared excitation measurement, the fundamental beam was directed onto the surface of a gold electrode in a spectroelectrochemical cell at an angle of incidence of 35°. The fluence of excitation was lower than 10 mJ per pulse. The SH light was separated from the fundamental laser beam with an IR-cut filter and a spectrometer (Ritu MC-10N) and detected by a photomultiplier tube (Hamamatsu R636). The incoming train of SH light pulses was averaged with a boxcar averager (Stanford Research SR250). The intensity and temporal profile of the fundamental beam were monitored by a separate reference channel and the SH signal was normalized at each laser shot. The reference channel consisted of a BBO crystal (Cleveland Crystals), filters and a fast photodiode. The polarization of the fundamental beam was set with a combination of a polarizer and a double Fresnel rhomb, and the polarization of the SH light was selected by another polarizer. All of the SHG data reported in this paper were obtained with the p-in/p-out polarization condition.

Two types of working electrode were used in this study: a 6 mm diameter polycrystalline gold disk that was embedded into a Teflon rod (for 585 nm excitation) and a 10 mm diameter polycrystalline gold disk that was held on a glass tube (for 1064 nm excitation). Because different types of holder were used, these electrodes were prepared by different methods. The former was mechanically polished with 0.05 μm alumina until optically flat and chemically cleaned in $\text{H}_2\text{O}_2 + \text{H}_2\text{SO}_4$ mixed solution before introduction into the spectroelectrochemical cell. These treatments yielded a sufficiently clean electrode surface. The latter was also mechanically polished with 0.3 μm alumina, and was then electrochemically polished for 30 min by sweeping the potential between -0.2 V and 1.5 V with a sweep rate of 0.5 V s^{-1} in 0.1 M HClO_4 solution in the spectroelectrochemical cell. A standard three-electrode configuration was constructed with a sodium saturated calomel electrode (SSCE) reference and a Pt counterelectrode. Millipore-filtered water was used in all experiments. Sodium perchlorate, perchloric acid and sulfuric acid were reagent grade and were used as received from Wako Pure Chemicals. The solution containing tellurium was prepared by dissolving TeO_2 (99.995%, Aldrich Chemicals) in concentrated perchloric acid prior to dilution. All the electrochemical measurements were carried out at room temperature

after deaeration of the solutions by bubbling with high purity nitrogen (better than 99.99%). The electrode potential was controlled with a potentiostat (Hokuto Denko HA-151) and a function generator (Hokuto Denko HB-111). The electrode potential, current and normalized SH intensity were captured digitally via an A/D converter and stored on a personal computer (NEC PC-9801VM).

Electrochemical SHG measurements were carried out in the following order. First, an electrochemical SHG measurement on a bare gold electrode was performed by sweeping the potential between -0.2 V and $+1.5$ V in 1 M H_2SO_4 or 0.1 M HClO_4 solution; then both the cyclic voltammogram (CV) and the potential dependence of SHG, typical of the clean gold electrode, were confirmed. After a clean gold surface was obtained, the solution containing tellurium was introduced into the spectroelectrochemical cell with nitrogen pressure. To prevent the adsorption of Te on the Au surface at the rest potential, the potential was kept at $+0.8$ V during exchange of the solution in the electrochemical cell. The electrode potential was then swept and SHG measurements were started.

In order to monitor the mass change at the Au surfaces during Te deposition, the EQCM method [37] was used. In the EQCM study, a gold thin film evaporated on a 5 MHz, AT-cut quartz plate was used as a working electrode. Details of the EQCM measurements have been described elsewhere [38].

3. Results and discussion

Fig. 1 shows the CV and the simultaneously obtained potential dependence of the 1064 nm excited SH signal from an Au surface in 0.1 M HClO_4 solution containing 0.5 mM TeO_2 . During the negative potential scan, a cathodic peak corresponding to the reduction of TeO_2 to

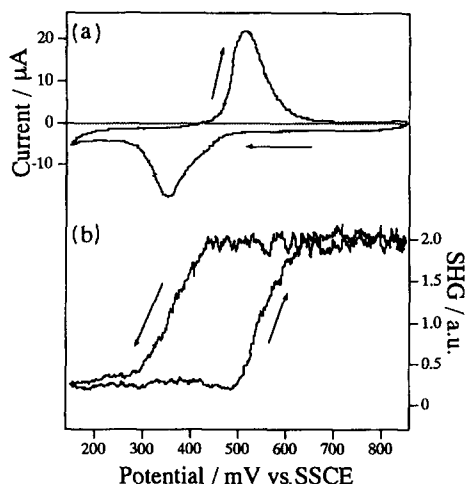


Fig. 1. (a) Cyclic voltammogram of first Te upd on gold electrode. Scan rate, 5 mV s^{-1} . (b) Potential dependence of 1064 nm excited SHG (532 nm) from gold surface spontaneously obtained with (a) (p-in/p-out).

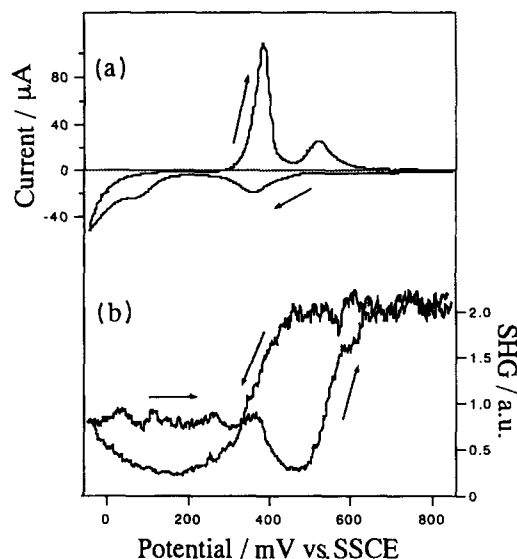
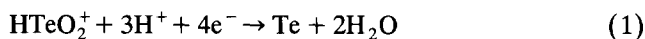


Fig. 2. (a) Cyclic voltammogram of upd and bulk deposition of Te on a gold electrode. Scan rate, 5 mV s^{-1} . (b) Potential dependence of 1064 nm excited SHG (532 nm) from a gold surface spontaneously obtained with (a) (p-in/p-out).

Te(0) was observed at 350 mV. It is referred to as the first upd peak. In the positive scan, a stripping peak of the first upd layer was observed at 520 mV. Similar CVs have been reported in previous studies using Au single crystal surfaces [10–13] and polycrystalline Au [8–10]. It is generally agreed that the reductive electrodeposition of TeO_2 to Te(0) occurs by the following four-electron reduction process



In this experiment, the potential was scanned up to 150 mV so that only the first Te upd was completed. For the negative potential scan, the SH signal decreased significantly as the first upd proceeded. In the positive scan, the SH signal increased as the desorption current of Te flowed, and the signal returned to its initial value after Te dissolution was completed, showing that the clean gold surface was recovered.

Fig. 2 shows the result of extending the potential window to more negative values. In addition to the first upd peak described above, the second upd peak, although only partially resolved from the bulk Te deposition current, appeared as a shoulder at 50 mV. In the positive scan, the stripping peak corresponding to the dissolution of bulk Te was observed at 350 mV. There was a small shoulder around 410 mV corresponding to the stripping of the second upd layer. A stripping peak of the first upd layer at 520 mV was clearly distinguishable from the peaks corresponding to the second upd and the bulk deposition of Te.

A significant decrease in SHG during the first Te upd was also observed. However, the SH intensity increased during the second Te upd and bulk Te deposition. The potential dependence of SHG, with and without TeO_2 in

solution, is compared in Fig. 3 for the negative potential sweep. Since only the monotonic decrease in 1064 nm excited SHG from the bare gold surface was observed during the negative potential scan [30,39], most of the variations of the SH intensity mentioned above were attributed to Te deposition.

In general, the SH intensity $I(2\omega)$ from a metal surface is proportional to the square of the complex surface second-order non-linear susceptibility $\chi_s^{(2)}$ and the square of the input light power $I(\omega)$ in the electric dipole approximation [14–16]

$$I(2\omega) \propto |e(2\omega) \cdot \chi_s^{(2)} \cdot e(\omega) \cdot e(\omega)|^2 I(\omega)^2 \quad (2)$$

where $e(\omega)$ and $e(2\omega)$ are the polarization vectors describing the input and output light fields. The surface non-linear susceptibility $\chi_s^{(2)}$ is modified by the presence of an adsorbate and becomes a new value, $\chi_s'^{(2)}$

$$\chi_s'^{(2)} = \chi_s^{(2)} + \chi_A^{(2)} + \Delta\chi_1^{(2)} \quad (3)$$

where $\chi_A^{(2)}$ is the inherent non-linear susceptibility of the adsorbate which is independent of the surface and $\Delta\chi_1^{(2)}$ is the perturbation in the non-linear susceptibility due to any interactions between the surface and the adsorbate. Although $\chi_s^{(2)}$ is usually larger than $\chi_A^{(2)}$ for metal surfaces, the non-linear optical properties of the Te-covered Au surface are not so simple, since the adsorbate (tellurium) absorbs photons in the wavelength region [37] employed in this study. Consequently, it is not clear whether the variations of SHG on Te deposition are due to the optical properties of the tellurium itself ($\chi_A^{(2)}$) or to the interaction between adsorbed Te and the Au substrate ($\Delta\chi_1^{(2)}$). Although $\chi_A^{(2)}$ is expected to be proportional to the amount of adsorbate, $\Delta\chi_1^{(2)}$ is not necessarily proportional to this value. The SHG behavior can be described by the linear function of the surface concentration of tellurium, Γ_{Te} , only when $\Delta\chi_1^{(2)}$ is proportional to Γ_{Te}

$$\chi_s'^{(2)} = \chi_s^{(2)}(1 + c\Gamma_{\text{Te}}) \quad (4)$$

where c is a proportionality constant, which is related to both $\chi_A^{(2)}$ and $\Delta\chi_1^{(2)}$. In this case, the following correlation is derived, since the SH signal is proportional to the square

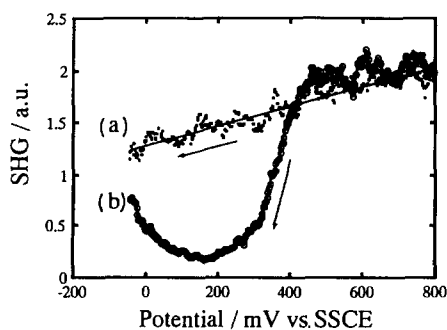


Fig. 3. SHG signal (excitation, 1064 nm) as a function of the potential of the Au electrode during a negative potential scan: (a) in 0.1 M HClO_4 (corresponding to $I(2\omega)_0$); (b) in 0.5 mM TeO_2 + 0.1 M HClO_4 (corresponding to $I(2\omega)$) (p-in/p-out). The full line is a linear least-squares fit.

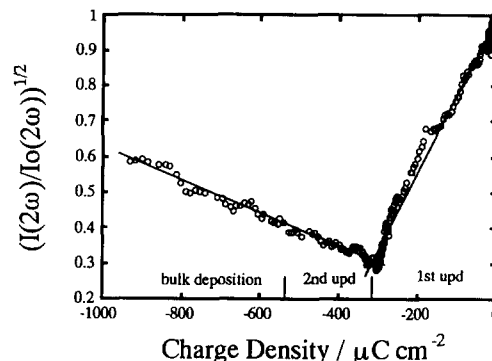


Fig. 4. Plot of the square root of the normalized SHG signal vs. the electric charge density for Te deposition (Q_{Te}) using Eq. (5); 1064 nm excitation. The full line is a linear least-squares fit. Details are described in the text.

of $\chi_s'^{(2)}$ and Γ_{Te} is derived from the Faradaic charge density Q_{Te} associated with Te deposition

$$\frac{\chi_s'^{(2)}}{\chi_s^{(2)}} \propto \left(\frac{I(2\omega)}{I(2\omega)_0} \right)^{1/2} = A + c'Q_{\text{Te}} \quad (5)$$

where $I(2\omega)_0$ is the SH intensity from the bare gold surface at each potential and c' is a proportionality constant affected by both the optical properties of adsorbed Te and adsorbate–substrate interactions.

Fig. 4 shows the $(I(2\omega)/I(2\omega)_0)$ vs. charge density (Q_{Te}) plot according to Eq. (5) for the Te deposition process presented in Fig. 2. To calculate the charge density for Te deposition, the double layer charging current was subtracted assuming that the current in the double layer region is independent of the potential. Since the SH signal from the bare gold surfaces ($I(2\omega)_0$) varied as a function of the electrode potential, the value $(I(2\omega)/I(2\omega)_0)^{1/2}$ was calculated at each potential. Fig. 4 clearly shows that there are two regions with different slopes. Regions I and II are associated with the first Te upd, and the second Te upd and bulk Te deposition regions respectively. The proportionality constant c' of Eq. (5) was determined to be 2.3×10^{-3} for region I and -6.8×10^{-4} for region II. A similar $(I(2\omega)/I(2\omega)_0)$ vs. charge density (Q_{Te}) plot was obtained for the desorption process of Te. Both the sign and magnitude of c' in region I are significantly different from those in region II, although tellurium atoms form a monolayer which adsorbs directly on the Au surface in both the first and second upd [13]. Consequently, there is a minimum of the SH intensity in the midst of the formation of the monoatomic layer of Te. In addition, the slope of the SH variation is the same, with no distinction between the second upd and bulk deposition of Te, although the adsorption sites are energetically different in each region. If the non-linear susceptibility of Te ($\chi_A^{(2)}$) is reflected in the SH signal, the SH intensity should vary monotonically with an increase in the surface concentration of Te and c' should be the same in both regions I and II. Accordingly, the sudden change in c' in the midst of the formation of

the monoatomic layer should be attributed mainly to the contribution of substrate–adsorbate interactions ($\Delta\chi_1^{(2)}$), and it is suggested that the interactions of the first upd Te and the second upd Te with the substrate are completely different.

The existence of a minimum of the SH intensity in the monolayer deposition region has been reported previously for Tl deposition on polycrystalline Ag electrodes [41,42]. This was attributed to Tl deposition occurring on energetically different sites in each deposition region [41]. This causes a stepwise variation of the non-linear susceptibility of the surface. However, the origin of the SH minimum was not discussed in detail. Furthermore, several different features of the SH behavior were noted. First, the slope of the SH variation for the bulk deposition of Tl on Ag was much larger than the slope for the monolayer region, suggesting that the SH behavior could reflect the transition from the monolayer adsorption region to the bulk deposition region. In the case of Te on Au, however, no such transition is evident. Second, in the case of Tl on Ag, the magnitude of c' was almost the same in the monolayer adsorption region, although the sign of c' changed in the midst of the upd process. In the case of Te on Au, the magnitude of c' in region I is at least three times larger than that in region II. These observations indicate that the modification mechanisms of the surface non-linear susceptibility are quite different for each case, and therefore other causes should be considered for Te deposition on Au.

In the present experimental conditions, the SH photons (2.33 eV) generated from the Au substrate are expected to couple with the interband transition because they are energetically accessible to the interband transition threshold for Au at 2.25 eV [24,43]. Therefore the SH signal from an Au surface should be enhanced significantly by this resonance. Thus it is probable that the decrease in the SH signal in the first Te upd region is due to the quenching of the resonantly enhanced surface non-/linear susceptibility of the Au substrate ($\chi_s^{(2)}$) by Te deposition. However, this cannot explain why the quenching of $\chi_s^{(2)}$ is complete on deposition of the first Te upd layer. Thus it is concluded that the influence of the first upd layer of Te on the surface electronic structure is larger than that of the second upd and bulk deposition layers.

As mentioned above, the interaction between the first Te upd layer and the Au substrate surface is distinctive, and such an interaction is interesting in view of the electronic properties of the surface. To examine the change in the surface electronic properties during the first Te deposition in more detail, the excitation wavelength was changed to 585 nm. At this excitation wavelength, the fundamental photon energy (2.1 eV) is slightly lower than the interband transition threshold of Au (2.25 eV), but the SH photon energy (4.2 eV) is much higher than that energy and other optical transitions may also take place. Thus the SH response was expected to be different from that on 1064 nm excitation.

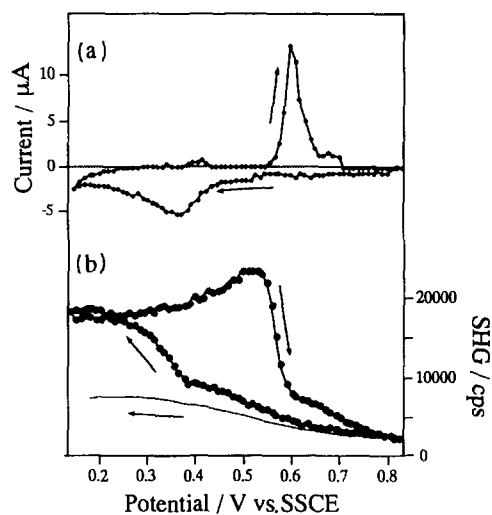


Fig. 5. Potential dependence of the current (a) and 585 nm excited SHG (292.5 nm) from the gold surface (b) in 0.5 mM TeO_2 + 0.1 M HClO_4 + 0.1 M NaClO_4 (scan rate, 10 mV per step; 1 s averaging; p-in/p-out). The lower curve represents the potential dependence of 585 nm excited SHG from the gold surface without Te deposition in 1 M H_2SO_4 .

Fig. 5 shows the potential dependence of the current and the 585 nm excited SH signal from an Au surface in 0.1 M HClO_4 + 0.1 M NaClO_4 aqueous solution containing 0.5 mM TeO_2 . The voltammogram is slightly different from Fig. 1(a) because a different electrode was used. As mentioned in Section 2, the history of the electrode used for Fig. 5(a) was different from that of the electrode used for Fig. 1(a). A separate experiment showed that the electrochemical cleaning cycle used for the electrode in Fig. 1(a) yielded a smaller peak separation of the voltammogram on Te upd, probably because of the increase in surface defects. Such differences in electrode preparation probably yield a different surface morphology and the morphology of the electrode surface affects the voltammograms of Te upd [13]. The potential dependence of the 585 nm excited SHG from bare Au in 1 M H_2SO_4 is also shown in Fig. 5 as the solid line. These results were obtained by averaging the SH signal for 1 s with every 10 mV potential step. At this excitation wavelength, SHG increased with the first Te upd, in contrast with the result obtained on 1064 nm excitation. This SH behavior obeys the linear correlation between the non-linear susceptibility and the surface coverage of Te as predicted by Eq. (5); this is shown in Fig. 6. In the positive scan, the SH signal continued to increase up to the potential at which the dissolution of the first upd layer started, although a cathodic current for Te deposition was not observed. Then the SH signal decreased sharply as the dissolution of the first Te upd layer proceeded. Thus the maximum of the SH signal appeared at the potential just before the dissolution of the first Te upd layer. The maximum became clearer when the electrode potential was swept more slowly. The gradual increase in SHG in the positive scan could not be explained by the linear correlation between the surface

non-linear susceptibility and the surface coverage of Te, because the deposition current for Te was not observed in the corresponding potential region.

The comparison between Figs. 1 and 5 shows clearly that the potential dependence of the SH intensity during the first Te upd process is dependent on the excitation wavelength. The deposition of Te on Au changes the SH signal in the opposite direction. Such a wavelength-dependent behavior of SHG was also observed in studies on the surface oxidation of gold electrodes: the SH intensity decreased with surface oxide formation on 1064 nm excitation, but increased with visible light excitation [30,39]. Both the optical properties of the gold substrate itself and the substrate-adsorbate interactions should be taken into account to understand fully this frequency-dependent behavior of SHG. When optical resonance with the electronic states of the substrate exists, free electrons and bound electrons, which take part in the electronic transition resonance, contribute to SHG, and the contribution to the induced non-linear polarization by the bound electrons should be dominant [44]. Thus we conclude that the adsorption of Te modifies the surface density of the bound electrons of Au. A more detailed quantitative explanation of the wavelength dependence of the SH behavior requires more data and a further development of the theory. Additionally, the gradual increase in the SH intensity before dissolution of the first Te upd layer is detected only on 585 nm excitation. Such a wavelength-dependent change in the SH intensity may be attributed to the perturbation of surface electronic properties.

One of the possible reasons for the electronic perturbation is the specific adsorption of anions. We carried out an EQCM measurement [37] to monitor the mass change at the electrode surface caused by anion adsorption. Fig. 7 shows the CV (a) and EQCM response (b) obtained simultaneously. Different features of the voltammogram (Fig. 7(a)) compared with those of Figs. 1(a) and 5(a) suggest that the evaporated Au electrode was oriented differently from the polycrystalline gold disk electrodes. In contrast

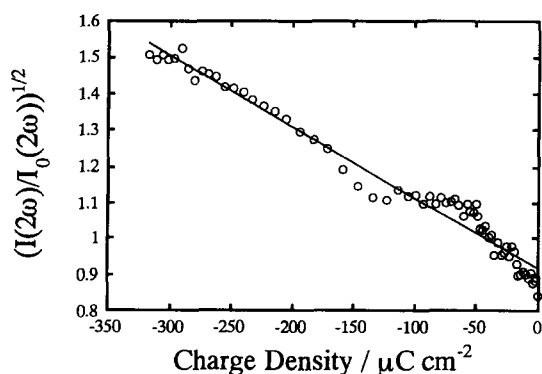


Fig. 6. Plot of the square root of the normalized SHG signal vs. the electric charge density for the first Te upd (Q_{Te}) using Eq. (5). The full line is a linear least-squares fit. Excitation, 585 nm. Details are described in the text.

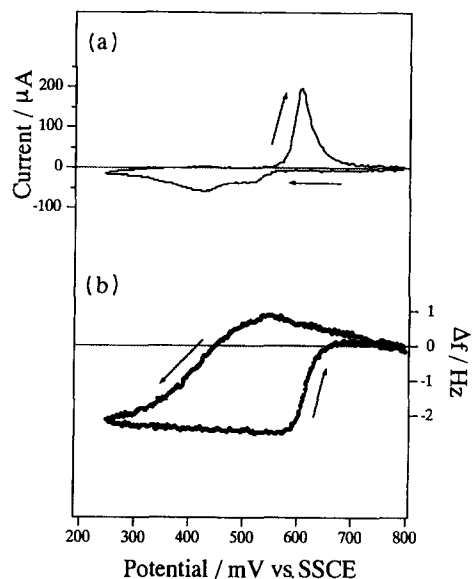


Fig. 7. (a) Cyclic voltammogram of first Te upd on gold electrode. (b) Potential dependence of resonant frequency shift (Δf) of 5 MHz EQCM. Both current and Δf were spontaneously obtained in 0.5 mM TeO_2 + 0.1 M HClO_4 . Scan rate, 20 mV s^{-1} .

with a previous EQCM study of Te deposition, where no mass change was observed during the first Te upd [8], valid mass changes during the first upd and dissolution processes were observed in the present study as shown in Fig. 7. These mass changes correspond to the Faradaic charge for deposited Te layers. As shown in Fig. 7, however, almost no frequency change of EQCM was observed in the potential region in which the gradual increase in SHG was observed. From these results, we conclude that anion adsorption is not responsible for the increase in SHG. This is consistent with the fact that the SH increase in the corresponding potential region is observed only on 585 nm excitation. Based on the results of STM measurements, Suggs and Stickney [13] suggested that Te dimer or chain structures were partially formed in the first Te upd layer, and the relative area of this domain structure increased as a function of the adsorption time and the electrode potential. The existence of Te-Te bonds should perturb the surface electronic properties and, in turn, modify the non-linear susceptibility of the surface. Thus the gradual increase in the SH signal in Fig. 5 may be attributed to the formation of in-plane Te-Te bonds. These explanations are consistent with the results of EQCM studies, which demonstrate that no mass change of the electrode occurs.

4. Conclusions

The in situ optical SHG technique was used to follow both the deposition and desorption processes of Te on polycrystalline Au electrodes. It was demonstrated that the SH signal was sufficiently sensitive to monolayer adsorp-

tion on metal surfaces and that the SHG study became more useful on changing the excitation wavelength. On 1064 nm excitation, the SH signal changed with the surface coverage of Te. It was also found that the first up layer of Te strongly perturbed the substrate surface. In contrast, on 585 nm excitation, the SH signal changed in a complicated fashion during the desorption process of the Te monolayer from Au. These results were interpreted in terms of the existence of an optical resonance and the gradual structural change which accompanies energetic perturbation on Te-covered Au surfaces.

Acknowledgements

The authors wish to thank Professor K. Shimazu for the loan of the EQCM equipment. This work was partially supported by the Grants-in-Aid for Scientific Research (04555191), Priority Area Research (05235201) and International Scientific Research (University-to-University Cooperative Research: 03045011) from the Ministry of Education and by the Kato Science Foundation and the Japan Science Society. I.Y. acknowledges the Japan Society for the Promotion of Science for a fellowship.

References

- [1] M.P.R. Panicker, M. Knaster and F.A. Kroger, *J. Electrochem. Soc.*, 125 (1978) 566.
- [2] (a) K. Uosaki, M. Takahashi and H. Kita, *Electrochim. Acta*, 29 (1984) 279; (b) M. Takahashi, K. Uosaki and H. Kita, *J. Electrochem. Soc.*, 131 (1984) 2304; (c) M. Takahashi, K. Uosaki and H. Kita, *J. Appl. Phys.*, 55 (1984) 3879.
- [3] J.H. Chen and C.C. Wan, *J. Electroanal. Chem.*, 365 (1994) 87.
- [4] R.W. Andrews, *Anal. Chim. Acta*, 119 (1980) 47.
- [5] R.S. Posey and R.W. Andrews, *Anal. Chim. Acta*, 119 (1980) 55.
- [6] J.M. Rosamilia and B. Miller, *J. Electroanal. Chem.*, 215 (1986) 261.
- [7] M. Traore, R. Modolo and O. Vittori, *Electrochim. Acta*, 33 (1988) 991.
- [8] E. Mori, C.K. Baker, J.R. Reynolds and K. Rajeshwar, *J. Electroanal. Chem.*, 252 (1988) 441.
- [9] B.W. Gregory and J.L. Stickney, *J. Electroanal. Chem.*, 300 (1991) 543.
- [10] B.W. Gregory, D.W. Suggs and J.L. Stickney, *J. Electrochem. Soc.*, 138 (1991) 1279.
- [11] D.W. Suggs and J.L. Stickney, *J. Phys. Chem.*, 95 (1991) 10 056.
- [12] D.W. Suggs and J.L. Stickney, *Surf. Sci.*, 290 (1993) 362.
- [13] D.W. Suggs and J.L. Stickney, *Surf. Sci.*, 290 (1993) 375.
- [14] P. Guyot-Sionnest, W. Chen and Y.R. Shen, *Phys. Rev. B*, 33 (1986) 8254.
- [15] R.M. Corn and D.A. Higgins, *Chem. Rev.*, 94 (1994) 107.
- [16] G.L. Richmond, J.M. Robinson and V.L. Shannon, *Prog. Surf. Sci.*, 28 (1988) 1.
- [17] D.J. Campbell and R.M. Corn, *J. Phys. Chem.*, 92 (1988) 5796.
- [18] T.D. Hewitt and D. Roy, *Chem. Phys. Lett.*, 181 (1991) 407.
- [19] M.L. Lynch, B.J. Barner and R.M. Corn, *J. Electroanal. Chem.*, 300 (1991) 447.
- [20] M.L. Lynch, B.J. Barner, J.M. Lantz and R.M. Corn, *J. Chim. Phys.*, 88 (1991) 1271.
- [21] A. Friedrich, B. Pettinger, D.M. Kolb, G. Lupke, R. Steinhoff and G. Marowsky, *Chem. Phys. Lett.*, 163 (1989) 123.
- [22] B. Pettinger, J. Lipkowski, S. Mirwald and A. Friedrich, *Surf. Sci.*, 269/270 (1992) 377.
- [23] D.A. Koos, V.L. Shannon and G.L. Richmond, *J. Phys. Chem.*, 94 (1990) 2091.
- [24] D.A. Koos and G.L. Richmond, *J. Phys. Chem.*, 96 (1992) 3770.
- [25] G. Petrocelli, S. Martellucci and R. Francini, *Appl. Phys. A*, (1993) 263.
- [26] T.E. Furtak, Y. Tang and L.I. Simpson, *Phys. Rev. B*, 46 (1992) 1719.
- [27] C.M. Li, L.E. Urbach and H.L. Dai, *Phys. Rev. B*, 49 (1994) 2104.
- [28] R. Georgiadis and G.L. Richmond, *J. Phys. Chem.*, 95 (1991) 2895.
- [29] R.A. Bradley, R. Georgiadis, S.D. Kevan and G.L. Richmond, *J. Chem. Phys.*, 99 (1993) 5535.
- [30] P. Guyot-Sionnest and A. Tadjeddine, *J. Chem. Phys.*, 92 (1990) 734.
- [31] M. Buck, F. Eisert and F. Trager, *Ber. Bunsenges. Phys. Chem.*, 97 (1993) 399.
- [32] T. Takamura, Y. Sato and K. Takamura, *J. Electroanal. Chem.*, 41 (1973) 31.
- [33] K. Takamura, F. Watanabe and T. Takamura, *Electrochim. Acta*, 26 (1981) 979.
- [34] R. Adzic, E. Yeager and B.D. Cahan, *J. Electrochem. Soc.*, 121 (1974) 474.
- [35] D.M. Kolb, D. Leutloff and M. Przasnyski, *Surf. Sci.*, 47 (1975) 622.
- [36] C.M. Mate, G.A. Somorjai, H.W.K. Tom, X.D. Zhu and Y.R. Shen, *J. Chem. Phys.*, 88 (1988) 441.
- [37] D.A. Buttry and M.D. Ward, *Chem. Rev.*, 92 (1992) 1355.
- [38] K. Shimazu and H. Kita, *J. Electroanal. Chem.*, 341 (1992) 361.
- [39] I. Yagi, S. Nakabayashi, K. Uosaki, J.M. Lantz and R.M. Corn, in preparation.
- [40] S. Tutihasi, G.G. Robert, R.C. Keeze and R.E. Drews, *Phys. Rev.*, 177 (1969) 1143.
- [41] J.M. Robinson and G.L. Richmond, *Chem. Phys.*, 141 (1990) 175.
- [42] J. Miraglietta and T.E. Furtak, *Phys. Rev. B*, 37 (1988) 1028.
- [43] J.D.E. McIntyre, in P. Dlahay and C.W. Tobias (Eds.), *Advances in Electrochemistry and Electrochemical Engineering*, Vol. 3, Wiley, New York, 1973, p. 61.
- [44] D. Roy, *Electrochim. Acta*, 36 (1994) 2699.